Performance Evaluation of a Hybrid PVT Solar Installation with Phase Change Material

Dr. Raquel Simón-Allué[1], Dr. Adriana Coca-Ortegón[1], Raúl Villén[1], Dr. Isabel Guedea[1]

[1] EndeF Engineering SL, Zaragoza (Spain)

Abstract

This paper evaluates the energy performance of an innovative solar installation composed of photovoltaic-thermal panels (PVT), half of which contain a layer of phase change material (PCM) within the panel. The main objective for the PCM inclusion is to provide an extra cooling effect to the PV laminate, as well as to take advantage of the excess heat produced during the hours of maximum sunshine and reallocate it at the end of the day. The solar circuit is completed with a stratified storage tank specially developed to work with multi-energy source while maximizing heat exploitation at low temperatures. The installation is located in the south of Spain and was designed in the frame of the European LowUP project (http://lowup-h2020.eu/) to provide electricity and heat to an office building. This work presents the analysis of the solar field during several months of operation.

Keywords: Solar energy, Photovoltaic-thermal (PVT), Phase change material, Field measurements

1. Introduction

Despite the effort of scientist, engineers, authorities and involved entities to improve the integration and efficiency of renewable systems, their contribution to final energy consumption remains low. According to statistics, only the 29.9% of the EU-28's total production of primary energy is from renewable energy sources (Eurostat, 2019) and it has fallen to 19.3% when the global world production is analyzed (REN21, 2017). If we focus on sectors, renewable energy met less than 14% in buildings and 14.5% of total energy demand industrial uses (REN21, 2020). In buildings in particular, more than three-quarters of the global final energy demand was for heating and cooling end uses, which remain largely fossil-fuel based. If we take into account the last restrictions (European Commission, 2019), an integrated approach for advancing both renewables and energy efficiency remains crucial.

In this frame, solar energy has a key role to play, as one of the most promising alternatives due to the abundant, inexhaustible and clean nature of the sun (Parida et al., 2011). As indicated in the last Global Status Report (REN21, 2020), solar energy was, together with wind, the renewable energy with the greatest projection in the energy market due to the decrease kWh cost. In the case of solar photovoltaics (PV), the market increased in a 12% in 2019, reaching to record figures, and experienced strong growth in the share of rooftop PV systems. However, solar energy still have some limitations, mainly related to low cell efficiencies, real economic profitability or government policies (Kabir et al., 2018; Karakaya and Sriwannawit, 2015). Further efforts are needed to achieve a better exploitation of solar energy and enable us its use it in new applications.

One way to improve the solar performance is to combine thermal and photovoltaic technologies on the same module, known as PVT panels (Besheer et al., 2016; Chow et al., 2012). The PVT collectors can generate both electricity and low-grade thermal energy during the daytime and have been widely studied during last decade (Aste et al., 2015; Buonomano et al., 2016; Jonas et al., 2019). Their relevance was pointed out by the International Energy Agency through the Task 60 of the Solar Heating & Cooling Programme (IEA-SCH, 2020), dedicated to PVT Systems and applications.

Due the mismatch between solar resource and heating demand, other relevant component in the solar systems is the energy storage technology. In the case of solar thermal installations, the most common options are Sensible Thermal Energy Storage Technologies (TES), using water storage tanks (Dincer and Rosen, 2011; Fertahi et al., 2018). Among the options used to improve the performance of this technology are the development of super-insulations, and the design of stratifier elements in order to reduce the mixing of fluids with different temperature levels (Andersen et al., 2007; Fertahi et al., 2018; Göppert et al., 2009; IEA, 2014).

An additional improvement is presented here through the addition of phase change material (PCM) within the PVT module. As widely known, phase change material (PCM) first absorbs sensible heat and when it reaches to

doi:10.18086/eurosun.2020.05.06 Available at http://proceedings.ises.org

its melting temperature, it absorbs latent heat. When the temperature goes down, it recovers the initial state while releases the heat stored. In the case of PVT solar collectors, it presents the twofold benefit of absorbing the excessive heat and reducing the PV working temperature.

Numerous works have focused on the benefits of PCM and solar combination from experimental (Islam et al., 2016; Mahamudul et al., 2016) to numerical point of view (Huang et al., 2007; Sarwar et al., 2011), mostly applied to separated thermal or PV panels. However, its integration on PVT collectors is scarcer, and just a few focus on the experimental behavior of PVT with PCM directly inserted (Browne et al., 2015; Preet et al., 2017; Yang et al., 2018), all of them related lab-testing experiments on traditional PVT collectors. To the author´s knowledge, there is a lack of studies about real installations working with PVT-PCM, which is exactly the goal of this work.

With a view to expanding this scope, this work presents the solar on-site performance of a demonstration plant which incorporates a novel PVT-PCM panel and a stratified storage tank with specific flow management to work with multi-energy source. The PVT-PCM collector was particularly developed for this purpose and placed next to the same model without PCM to evaluate the improvement derived from the PCM insertion. This installation works under real environmental conditions to provide electricity and cover heating needs from an office building.

2. Description of the installation

This installation takes part of one of the four demonstration plants developed within the framework of the LowUP project ("LowUP," 2020), with the aim of developing low temperature heat supply systems (30-35ºC) generated by renewable energy sources and use of wastewater. This particular solar installation is located in Seville, south of Spain, with the main objective of providing electricity and heat for heating (low temperature radiant floor) to an office building.

Solar field is composed by 40 photovoltaic-thermal (PVT) panels distributed in eight benches of five panels, and separated in two parallel lines (see Fig. 1): one with 20 plain PVT panels (Line w/o PCM) and second with 20 PVT panels with a layer of phase-change material (PCM) inserted (Line w/ PCM). Panels are hydraulically connected in parallel via Tichelmann loop. All panels are installed facing south (0º) with a tilt of 45º, to intensify the energy production in winter.

Fig. 1: Physical arrangement of the solar field (left) and stratified storage tank (right).

The entire plant is originally designed to operate with several low temperature sources (LTS: solar field, sewage water) and low temperature loads (LTL: radiant floor, dry cooler). However, to better analyze the contribution of the solar components, only one source (solar field) and one load (radiant floor) have been studied.

2.1. PVT collectors and PCM

The internal configuration of PVT panels was developed in the first age of the project, where their design was selected from several options. Due to the extreme climate of Seville and the low temperature needed for the supply, all PVT panels are unglazed. They incorporate a 60-cell 275W polycrystalline PV module (A_G=1.65 m^2, A_{PV}=1.56 m^2), together with an aluminum absorber through which the exchange fluid flows. In the case of the PVT-PCM line, panels incorporate a layer of PCM in direct contact with the heat absorber to remove the surplus heat. All panels are closed with a 25-mm layer of insulation and a metal rear sheet.

The initial objective of the inclusion of PCM was to control the excess of heat generated in the PVT, limit the maximum temperature of the PV and store the heat generated with a temperature higher than the required for the

thermal load (40ºC). Thus, the melting range selected for this application was 48ºC, greater than other PCMs found in literature for solar applications (Atkin and Farid, 2015; Hasan et al., 2010; Ma et al., 2015).

The PCM used for this application was inorganic, a salt hydrate type C48 from ClimSEL™ line (Fig. 2, melting temperature point: 48°C, melting latent heat:180 kJ/kg and density: 1300 kg/m3) (ClimSel C48, 2017). In order to prevent hybrid collector units from possible PCM leaks during the liquid state, PCM was added to the panel in individual packages covered by an external aluminium foil enclosure. Each pouch contained 0.5 kg of PCM and had a dimension of 125x300x10 mm. A total of 32 PCM packages (16 kg) were located inside each PVT panel, between the heat absorber and the insulation, forming a grid of 4x8 PCM elements. The result was a 10 mm PCM layer covering more than 80% of the absorber surface, where the heat is transferred by conduction, from the heat fluid to the PCM or vice versa.

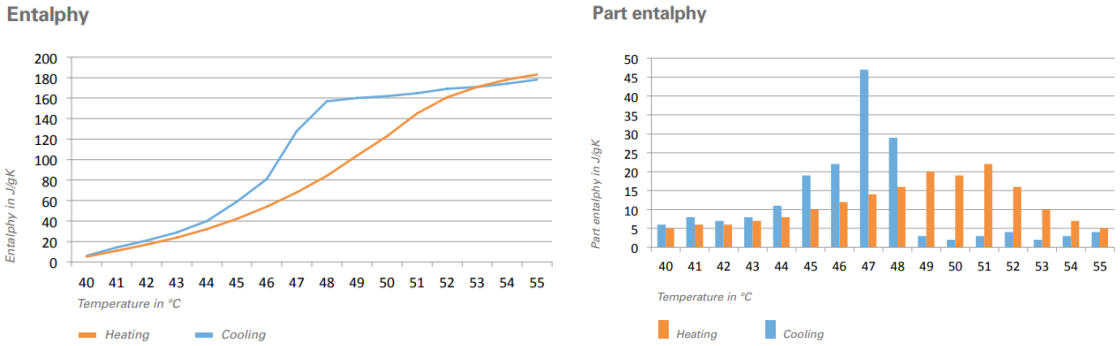

Fig. 2: Enthalpy and partial enthalpy absorbed and released by the PCM according to datasheet (ClimSel C48, 2017). Performance during melting (orange) and during crystallization (blue).

A redesign of the PVT assembly was also carried out to minimize the panel size, reduce labor time and facilitate the installation process. Further information about the manufacturing process and experimental testing of the PVT panels can be found in Simón-Allué et al. 2019.

2.1. Stratified storage tank

Due to the characteristics of the installation, with several low temperature sources (LTS) and low temperature loads (LTL), a particular thermal water storage tank was developed within the framework of the project, with a total volume of 6630l. The tank includes different stratifying elements, which contribute to not mixing fluids at different temperatures, thus improving the energy and exergetic efficiency of the installation. These stratifying elements are the following: a stratification column for a low temperature heat source (LTS), in this case, solar energy (Fig. 3 (a)); a second stratification column; which receives the return of a low temperature thermal load (LTL), in this case, the radiant floor from the office building (Fig. 3 (b)); and finally, two horizontal diffusers, designed to distribute the heat coming from a second low-temperature heat source, in this case a heat pump (Fig. 3 (c)).

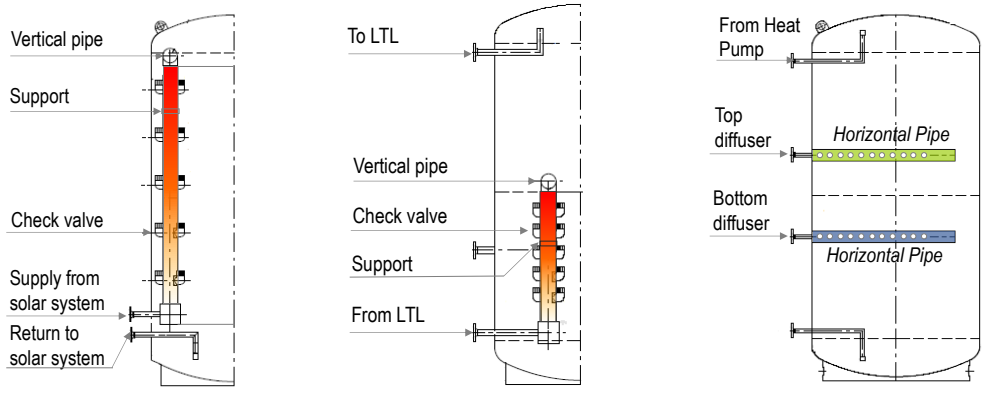

(a) Stratifying column for Low Temperature Source (LTS)

(b) Stratifying column for Low Temperature Load (LTL)

(c) Horizontal diffusers

Fig. 3: Stratified elements inside of thermal water tank.

The stratification columns consist of a collector tube, placed in a vertical position inside the thermal storage tank, with a set of check valves installed along the column. These valves cause a low-pressure drop in the system and regulate their state (open/close) with regard to the pressure difference between inside and outside of the collector, thus allowing the fluid to be introduced the tank according to the temperature level.

In order to monitor the tank-stratification, a total of 12 temperature sensors, type PT100, were installed inside the tank, distributed vertically.

2.2. Other components

Electrical circuit accounts on a three-phase 10 kW solar inverter, from the SMA Sunny Tripower line. Besides, the hydraulic circuit is completed with a heat sink (Inditer ATS-391 32 kW) to evacuate heat in case of necessity, two expansion vessels (20L each) to absorb expansion of the fluid and a circulating pump (Wilo Stratus DN 40 1/16).

Solar field is equipped with a complete list of sensors to favor monitoring of the energy generation, including temperature sensors, pressure valves, flow meters and electrical gauge. A weather station is also included with a pyranometer and anemometer to measure solar radiation and air velocity on field.

Additional temperature sensors are included in the inlet and outlet of each bench and inside panels with and without PCM, to better assess the PCM performance during operation. In the case of panels without PCM, three temperature probes are located between the heat absorber and the rear insulation, at the bottom (next to the inlet), middle and top (next to the outlet) of the panel. In the case of panels with PCM, three probes are located between the heat absorber and PCM packages at the bottom (next to the inlet), middle and top (next to the outlet) of the panel, and two more between PCM packages and back insulation at the bottom (next to the inlet) and top (next to the outlet) of the panel.

3. Testing conditions

The installation has been running during the summer months of Spain, corresponding to May to August. For this study, two working modes have been analysed, with and without heating loads. In both working modes, solar field operates by transferring heat to the stratified storage tank.

- Mode #1: solar field + stratified tank, operating with heating loads

In this mode two cases are analysed: when the heating load (HL) is produced during the daylight, matching the solar generation, and when the HL is produced at the end of the day, displaced from the solar generation.

- Mode #2: solar field + stratified tank, operating without heating loads

In this mode three cases are analysed, depending on the temperature storage tank at the beginning of the day. Since there is no thermal load applied to the storage tank, the starting temperature of the water storage directly modifies the operation of the solar field. Thus, three cases are studied considering cold tank (T_m ~25ºC), warm tank (T_m ~42ºC) and hot tank (T_m ~52ºC),

The control of the installation is performed based on the fluid temperature in the outlet of the solar field. Since the plant is designed to provide heat for heating purposes, specifically a low temperature radiant floor which operates below 40ºC, the solar field is regulated to provide an outlet fluid temperature of 45ºC. When the solar circuit is under this value, the pump reduces the rate flow in steps up to reach the minimum flow (25% of the nominal flow) in order to increase the outlet temperature of the panels. When the solar circuit is above this temperature, the pump increases the rate flow up to reach the nominal flow. The nominal flow value considered in the solar circuit is 40 l/(h·m2), which makes a total of 1.250 l/h per line (with and without PCM).

All tests have been performed on days with clear sky, under similar environmental conditions.

4. Performance indicators

To evaluate and compare the performance of each line (with and without PCM) when working in the two operating modes (with and without heating loads), we have calculated several performance indicators here described.

4.1. PVT collectors

Both thermal and electrical daily power production are quantified. However, in order to avoid deviations resulting from small variations of the solar irradiance, thermal and electrical efficiencies are used to compare results on different cases.

The thermal power (in Watts) generated by each line is calculated based on the fluid flow rate ($\dot{m}_{line}$) and the thermal gap of the fluid in its path through the 20 collectors of each line (eq. 1). Then, the instantaneous thermal efficiency is calculated considering the irradiation on the collector plane (in W/m2) and the total solar surface of the line ($A_{G,TOT} = A_G \cdot 20$ panels) (eq. 2).

$$\dot{Q}_{th} = \dot{m}_{line} \cdot c_f \cdot \Delta T \qquad \text{eq. 1}$$

$$\eta_{th} = \frac{\dot{Q}_{th}}{(A_{G,TOT} \cdot G)} \qquad \text{eq. 2}$$

Following same procedure, instantaneous electrical efficiency is calculated based on the instantaneous electrical output (P_e) and the total photovoltaic surface of the line ($_{APV,TOT} = A_{PV} \cdot 20$ panels) (eq. 3).

$$\eta_{PV} = \frac{P_e}{(A_{PV,TOT} \cdot G)} \qquad \text{eq. 3}$$

Total PVT efficiency of each line is calculated through the direct addition of the thermal and electrical efficiencies, given by eq. 4, where ζ is the blanketing factor, corresponding to the quotient between the photovoltaic and the gross area of the PVT, $\zeta = A_{PV}/A_G$ (Huang et al., 2001; Yang et al., 2018). For these panels, ζ takes the value of 0,945.

$$\eta_{TOT,line} = \eta_{th,line} + \zeta \cdot \eta_{e,line} \qquad \text{eq. 4}$$

Total amount of thermal (Q) and electrical energy (E) generated during the day by each line are also calculated based on the power and the daily operation time for the thermal and electrical circuit, respectively. Then, daily efficiencies are calculated as indicated in eq. 5 and eq. 6, being I the total radiation incident on each line during the whole day.

$$\overline{\eta_{th}} = {}^{Q}/_{I} \qquad \text{eq. 5}$$

$$\overline{\eta_{PV}} = {}^{E}/_{I} \qquad \text{eq. 6}$$

4.2. Storage indicators

The potential of the PCM is directly related to the temperature reached inside the PVT collectors. In order to be able to compare both cases, two parameters are calculated.

First, the total amount of heat released by the PCM (Q_{PCM}) is calculated based on the difference between the thermal energy generated in the line with and without PCM, measured when the solar field is lowering temperature and starts working below 48ºC (Fig. 2, melting PCM point). This time period varies from each case.

The melting factor (estimation of the amount of PCM melted based on the energy released) is calculated as indicates in eq. 7, where LH is the latent heat of the PCM (180 kJ/kg) and QTY_{PCM} the amount of PCM inserted in the PCM line (320kg).

$$MF_{PCM} = \frac{Q_{PCM}}{(LH \cdot QTY_{PCM})} = \frac{(Q_{PCM\ line} - Q_{PVT\ line})_{blw\ 48ºC}}{(LH \cdot QTY_{PCM})} \quad \text{eq. 7}$$

The tank-stratification is evaluated during the charging process, through the vertical temperature profile evolution, obtained from the 12 temperature sensors installed inside the tank. During this charging process, the maximum temperature difference inside the tank ($\Delta T_{ST,\ MAX}$) is calculated according to eq. 8.

$$\Delta T_{ST,MAX} = T_{top} - T_{bottom} \quad \text{eq. 8}$$

Other complementary stratification indicators, based on variables such us, Moment of Energy (M), calculated for each layer inside of tank (Andersen, 2007, p. 1220), are outside the scope of this paper.

5. Results & discussion

Environmental conditions of the different testing days are gathered in Tab. 1. In order to focus on the most relevant time period, average values have been calculated from data registered from 11 to 6 pm, which matches the time slot with maximum solar radiation. In this table, average data corresponding to the solar irradiance on the collector plane (G_m), environmental temperature (Ta_m) and wind speed on collector plane (Wind SP_m) are presented.

Tab. 1: Average values (from 11 to 6 pm) of environmental conditions given on testing days.

Mode	Case	G_m (W/m2)	Ta_m (ºC)	Wind SP_m (m/s)
#1	HL 2 to 8 pm	698	29,3	0,82
	HL 7 pm to midnight	682	33,0	0,95
#2	Cold Tank	687	26,2	0,77
	Warm Tank	710	31,1	1,64
	Hot Tank	709	35,7	1,02

Mean values of solar irradiance seem to be slightly low considering the high solar radiation of the south of Spain. However, it should be remarked the G_m value is calculated on the collector plane, with in this case it has a tilt of 45º. This angle is 8º over the latitude of Seville (37º) and was selected to emphasize the power generation during winter, but that entails a lowering of the radiation received on the plane during the summer. With this in mind, G_m values are logical.

5.1. Mode #1: Solar field with heating load

Daily profile of power generation and instantaneous efficiencies when the installation is working with heating loads during the daylight are presented in Fig. 4. On the left vertical axis, this figure shows the thermal (continuous lines) and electrical power (double line) for lines with (dark purple) and without PCM (green) as well as the solar radiation incident over each 20-panels line. On the right vertical axis, the figure includes total efficiencies calculated as indicated in eq. 4. To complete the information, temperature daily profiles are also provided in Fig. 5, showing temperature data at the inlet and outlet of each line (left) and inside the storage tank (right).

Based on these figures, the inclusion of PCM inside the panels leads to an increase in the thermal and electrical power during the day. At the beginning of the day (up to 12pm), the thermal generation of the line with PCM remains slightly lower than the line without, due to the inertia provoked by the PCM consumes part of the heat generated by heating the PCM instead of the fluid. After midday, the solar field begins to provide heat to the storage tank and increases the gap between inlet/outlet temperatures of solar collectors. At 2 pm, the heating load starts to remove heat from the lower layers of the storage tank. Since the thermal loads are not much higher than the solar generation, the higher layers of the tank continue to accumulate solar heat, favoring stratification. The maximum gap found in the storage tank during the charging process rises up to 13ºC. In the solar circuit, the fluid reaches temperatures of 50ºC in the outlet of the collector, which allows us to assume that the layer of PCM in contact with the heat absorber has started to melt.

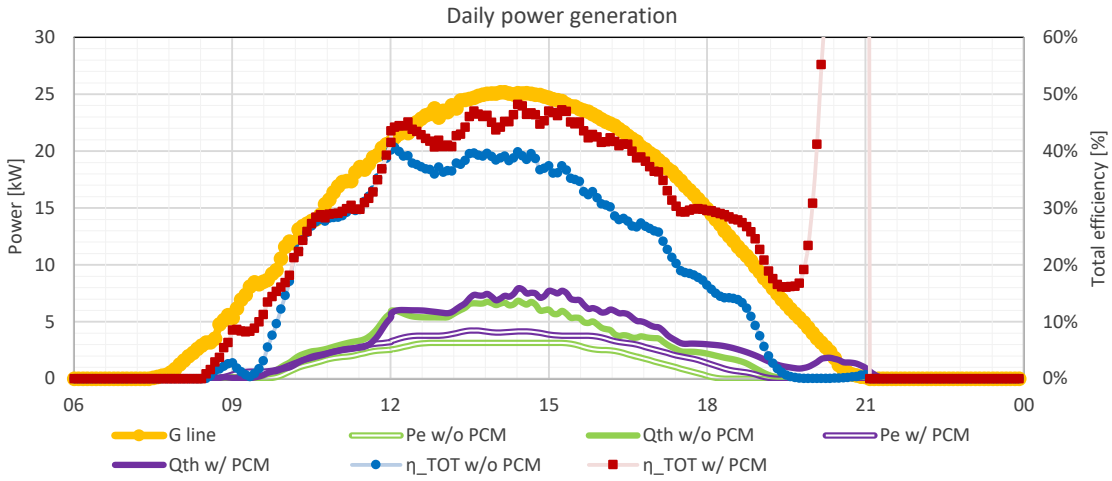

Fig. 4: Power generation and total efficiency daily profile in Mode #1, heating load from 2pm to 8 pm.

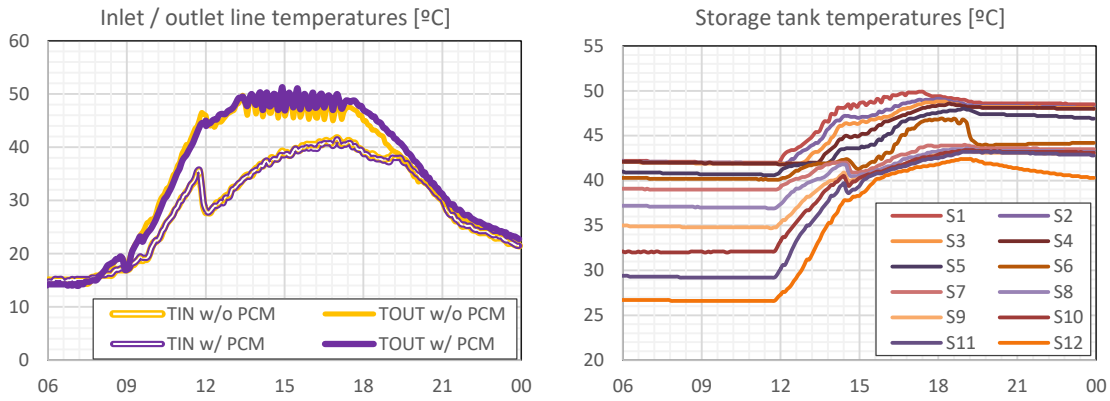

Fig. 5: Temperature daily profile in the inlet/outlet lines (left) and storage stratification (right) in Mode #1, heating load from 2pm to 8 pm.

Instant efficiencies reflect the pattern followed by the thermal and electrical power generation, showing a higher value for the line with PCM than the line without. At the end of the day, it is noticeable a peak on the efficiency of the PCM line, due to the late thermal energy produced in this line at the end of the day. This thermal power is not resulting from the sun radiation, but from the heat stored in the PCM, so it has no sense to relate it directly to the solar radiation. These efficiency values are not considered in the study.

Contrary to expectations, the use of PCM does not lead to a reduction of the operating fluid temperature, which keep quite similar in both lines (Fig. 5, left). However, higher electrical efficiencies are found in the PCM line versus the plain PVT line, which indicates a significant difference on the cell temperature (around 0.5% each ºC, according to literature). At this point, it should be remarked that the operating temperature is measured based on the fluid temperatures, but not the PV cell temperatures, which are substantially lower.

Our assumption is that the inclusion of PCM favors the heat transmission from the PV laminate to the heat absorber and the PCM layer, making the PV cell work in a lower temperature and transferring more heat to the fluid. This better transmission (made by conduction) may be the result of adding one more metallic layer to which the heat passes, or that the assembly of the components within the PVT with PCM has been carried out with higher pressure in the manufacturing phase (to include an extra layer of 10mm into the same space) that maximizes the contact. The consequence of this better heat transmission would be the reduction of the PV temperature but the increase on the PCM layer, which would result in a similar operating temperature of the fluid. This assumption may explain the increase on the instantaneous thermal and electrical efficiencies for the line with PCM.

When similar heating load is scheduled during the evening, the system works as there was no heating load during daylight, and heat generated in the solar field is only stored in the tank. In this case, the stratification capacity of

the tank keeps very limited due to the continuous charging process and the maximum temperature gap between top and bottom layers round 5ºC (see Fig. 6, right).

Since the system is not able to evacuate heat up to 7pm, both the tank and the solar circuit work in a higher operating temperature (Fig. 6, left), which provokes a greater amount of PCM melted. The PCM releases the energy stored when the solar circuit starts lowering temperature at the end of the day, coinciding in time with the activation of the heating load, which makes it possible to make use of the heat generated. As a result, the thermal improvement provoked by this case is higher than others.

The addition of PCM causes an improvement of around 4% in the PV performance and between 2 to 9% in the thermal performance, for cases with daily or evening heating load.

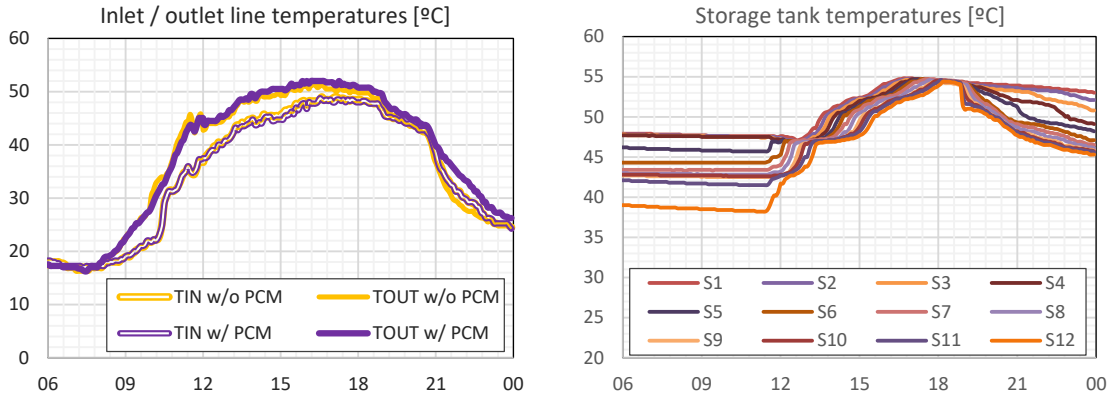

Fig. 6: Temperature daily profile in the inlet/outlet lines (left) and storage stratification (right) in Mode #1, heating loads from 7 pm to midnight.

Tab. 2: Main performance values for Mode #1, when the heating load is produced during the daylight (from 2pm to 8pm) and during the evening (from 7pm to midnight).

Heating load	Line	$T_{op,m}$ (11 – 6 pm)	$\eta_{th,m}$ (11 – 6 pm)	$\eta_{PV,m}$ (11 – 6 pm)	$\Delta T_{ST,MAX}$	$\overline{\eta_{th}}$	$\overline{\eta_{PV}}$	MF_{PCM}
2 pm to 8 pm	w/o PCM	41.3	21.8 %	11.1 %	13ºC	20.3 %	11.3 %	-
	w/ PCM	41.6	25.0 %	15.2 %		24.6 %	14.4 %	23%
7 pm to midnight	w/o PCM	45.9	22.3 %	10.0 %	5 ºC	22.5 %	10.2 %	-
	w/ PCM	45.8	28.9 %	14.4 %		31.4 %	13.7 %	35%

5.2. Mode #2: Solar field without heating load

When there are no thermal loads during the day, the capacity of the thermal tank to store heat becomes paramount, which is directly dependent on the storage temperature at the beginning of the test. Therefore, comparison at different storage temperatures is included. Main performance data are collected in Tab. 3.

When the starting temperature of the storage tank is low (below operating temperature of the solar circuit), the tank capacity to store energy is high, as it is also the temperature gap between inlet and outlet in the solar field (Fig. 7, left). However, to reach the objective temperature, the system needs to work with lower fluid flow, so the thermal generation is limited. The great stratification capacity of the tank is very visible here, reaching to maximum temperature difference inside the tank of 17ºC (Fig. 7, right).

In this case, thermal and electrical efficiencies (see Tab. 3) are similar to those values found in Mode #1, with daily heating load. This happens because the storage tank is able to store all the heat generated by the solar field, so the absence of load is not noticeable.

When the storage tank is heated, it becomes more difficult for the tank to store all the heat generated in the solar field. The stratification capacity of the tank is minimal and all the layers end with the same temperature (Fig. 8). This forces the solar circuit to operate at a higher temperature, which reduces general efficiencies but increases

the amount of PCM melted during the day, intensifying its effect at the end of the day. At this point, the storage capacity of the PCM becomes more relevant.

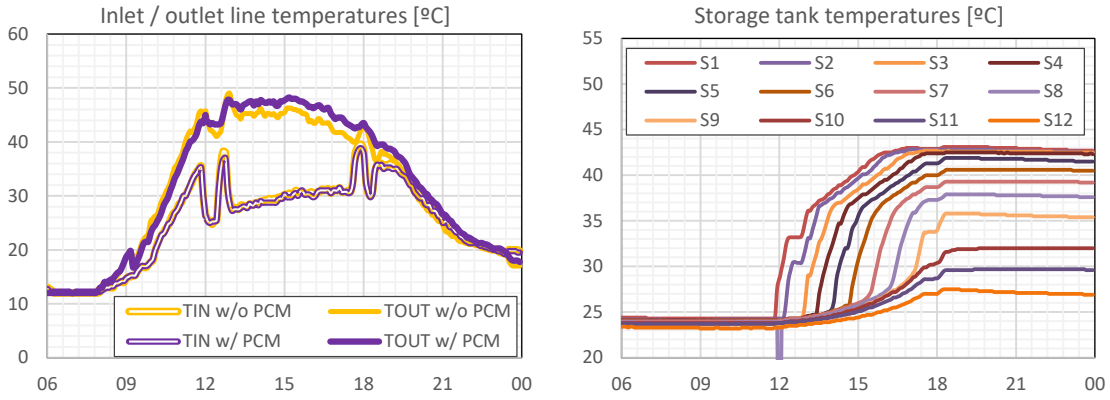

Fig. 7: Temperature daily profile in the inlet/outlet lines (left) and storage stratification (right) in Mode #2, cold tank.

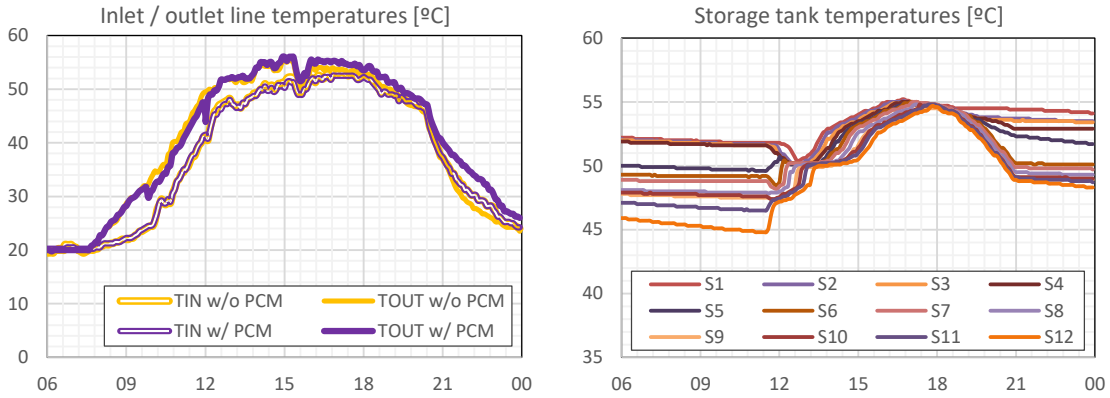

Fig. 8: Temperature daily profile in the inlet/outlet lines (left) and storage stratification (right) in Mode #2, hot tank.

Tab. 3: Main performance values for Mode #2, without heating loads.

Case	Line	Tm (11 – 6 pm)	$\eta_{th,m}$ (11 – 6 pm)	$\eta_{PV,m}$ (11 – 6 pm)	$\Delta T_{ST,MAX}$	$\overline{\eta_{th}}$	$\overline{\eta_{PV}}$	MF_{PCM}
Cold Tank	w/o PCM	37.2	21.8 %	11.9 %	17.3	20.3 %	11.9 %	-
	w/ PCM	37.7	24.9 %	15.3 %		23.7 %	14.3 %	12%
Warm Tank	w/o PCM	43.4	19.3 %	10.3 %	4.4	18.0 %	9.8 %	-
	w/ PCM	43.4	28.6 %	14.3 %		27.9 %	13.3 %	31%
Hot Tank	w/o PCM	49.9	16.5 %	9.3 %	4.1	15.3 %	9.3 %	-
	w/ PCM	49.9	23.0 %	13.7 %		25.8 %	12.8 %	56%

If we compare lines without PCM, the instantaneous thermal and electrical efficiencies decrease while the internal tank temperature and therefore, the operating temperature of the solar circuit increases (see Tab. 3). The same is true for the daily efficiencies and the electrical side of PCM line.

However, if we compare thermal performance of lines with PCM the analysis goes more complicated. When the tank is cold, the inlet temperature of the solar circuit is cooler than other cases, so as the medium temperature of the PVT+PCM collectors. This provokes that only a small part of the PCM is melted and the effect in the thermal

generation remains low. When the tank is warm, however, the effect of the PCM gains importance while the operation temperature is still not very high. As a consequence, the instantaneous efficiency increases, as well as the daily one, which takes into account the thermal generation at the end of the day. When the tank is too hot, as in the third case, the amount of PCM melted is maximum, but the high operating temperature of the solar circuit decreases the thermal performance versus the other two cases. The daily thermal efficiency $\overline{\eta_{th}}$ still remains higher than in the case of cold tank, because it takes into account the energy stored in the PCM melted and released at the end of the day.

The addition of PCM entails an improvement of around 4% in the PV performance and between 3 to 10% in the thermal performance, for cold to hot tank cases, respectively.

6. Conclusions

From the data exposed in this work, we can obtain several main conclusions.

- The use of PCM did not lead to a reduction on the fluid temperature, contrary to that exposed in literature. It may be explained because the PCM used in this case has a melting point (48ºC) much higher than other studies (ranged between 20-30ºC), and then the PVT solar field is not able to work for a long time over this temperature to provoked a reduction in the operating temperature.
- However, the addition of PCM provokes significant improvements in the thermal and electrical performance of the solar circuit, with direct influence not only in the energy generated at the end of the day, but also in the instantaneous efficiencies. This efficiency improvement may be explained due to a better heat transmission from the PV cell to the to the heat absorber and the PCM layer, which would reduce the PV cell temperature but increase the PCM layer, resulting in similar fluid temperatures. This improvement is more noticeable when the solar circuit works in a higher temperature, since more amount of PCM is activated.
- The sensitive thermal storage tank helps to properly manage low-temperature heat sources, such as solar energy from PVT collectors. When the demand takes place throughout the day, as is usual in offices, the stratification of the tank is maintained and allows a better use of the energy produced. When the demand takes place at the end of the day, the stratification is lower, but the tank reaches higher temperatures, storing more thermal energy for its later.
- The great volume of the storage tank, as well as the stratification capacity, hinders the absence of heating demand and allows the solar circuit to operate with acceptable efficiencies, comparable to those obtained with heat evacuation. In case of high temperature, this storage capacity of the tank is endorsed by the storage capability of the PCM.

Although further analysis is recommended to fully address and quantify the benefits of PCM in a PVT solar installation, this work provides reliable data of a PVT+PCM installation working under real conditions where the addition of PCM showed an undeniable improvement. Further studies are needed to evaluate the goodness of the installation in other climate conditions (winter) or different points of view (economical, environmental).

7. Acknowledgments

This work takes part of the LowUp project (*LOW valued energy sources UPgrading for buildings and industry uses)* which has received funding from the European Union's Horizon 2020 Research and Innovation Program under Grant Agreement n°723930.

8. References

Andersen, E., Furbo, S., Fan, J., 2007. Multilayer fabric stratification pipes for solar tanks. Sol. Energy 81, 1219–1226. https://doi.org/10.1016/j.solener.2007.01.008

Aste, N., Leonforte, F., Del Pero, C., 2015. Design, modeling and performance monitoring of a photovoltaic-thermal (PVT) water collector. Sol. Energy 112, 85–99. https://doi.org/10.1016/j.solener.2014.11.025

Atkin, P., Farid, M.M., 2015. Improving the efficiency of photovoltaic cells using PCM infused graphite and

aluminium fins. Sol. Energy 114, 217–228. https://doi.org/10.1016/j.solener.2015.01.037

Besheer, A.H., Smyth, M., Zacharopoulos, A., Mondol, J., Pugsley, A., 2016. Review on recent approaches for hybrid PV/T solar technology. Int. J. Energy Res. 40, 2038–2053. https://doi.org/10.1002/er.3567

Browne, M.C., Lawlor, K., Kelly, A., Norton, B., Cormack, S.J.M., 2015. Indoor Characterisation of a Photovoltaic/ Thermal Phase Change Material System. Energy Procedia 70, 163–171. https://doi.org/10.1016/j.egypro.2015.02.112

Buonomano, A., Calise, F., Vicidomini, M., 2016. Design, simulation and experimental investigation of a solar system based on PV panels and PVT collectors. Energies 9, 1–17. https://doi.org/10.3390/en9070497

Chow, T.T., Tiwari, G.N., Menezo, C., 2012. Hybrid solar: A review on photovoltaic and thermal power integration. Int. J. Photoenergy 2012. https://doi.org/10.1155/2012/307287

ClimSel C48, 2017. Product specification sheet.

Dincer, I., Rosen, M.A., 2011. Thermal energy storage. Systems and applications, 2nd ed. Wiley. A John Wiley and Sons, Ltd., UK.

European Commission, 2019. European Green Deal, EU Climate Action. Belgium. https://doi.org/10.1017/CBO9781107415324.004

Eurostat, 2019. Energy, Transport and environment statistics. 2019 edition. Luxembourg. https://doi.org/10.2785/660147

Fertahi, S. ed D., Jamil, A., Benbassou, A., 2018. Review on Solar Thermal Stratified Storage Tanks (STSST): Insight on stratification studies and efficiency indicators. Sol. Energy 176, 126–145. https://doi.org/10.1016/j.solener.2018.10.028

Göppert, S., Lohse, R., Urbaneck, T., Schirmer, U., Platzer, B., Steinert, P., 2009. New computation method for stratification pipes of solar storage tanks. Sol. Energy 83, 1578–1587. https://doi.org/10.1016/j.solener.2009.05.007

Hasan, A., Mccormack, S.J., Huang, M.J., Norton, B., 2010. Evaluation of phase change materials for thermal regulation enhancement of building integrated photovoltaics. Sol. Energy 84, 1601–1612. https://doi.org/10.1016/j.solener.2010.06.010

Huang, B.J., Lin, T.H., Hung, W.C., Sun, F.S., 2001. Performance evaluation of solar photovoltaic / thermal systems. Sol. Energy 70, 443–448. https://doi.org/10.1016/S0038-092X(00)00153-5

Huang, M.J., Eames, P.C., Norton, B., 2007. Comparison of Predictions Made Using a New 3D Phase Change Material Thermal Control Model with Experimental Measurements and Predictions Made Using a Validated 2D Model. Heat Transf. Eng. 28, 31–37. https://doi.org/10.1080/01457630600985634

IEA-SCH, 2020. Task 60 [WWW Document]. PVT Syst. Appl. PVT Collect. New Solut. HVAC Syst. URL https://task60.iea-shc.org/ (accessed 11.8.20).

IEA, 2014. Technology Roadmap Energy Storage. https://doi.org/10.1007/springerreference_7300

Islam, M.M., Pandey, A.K., Hasanuzzaman, M., Rahim, N.A., 2016. Recent progresses and achievements in photovoltaic-phase change material technology: A review with special treatment on photovoltaic thermal-phase change material systems. Energy Convers. Manag. 126, 177–204. https://doi.org/10.1016/j.enconman.2016.07.075

Jonas, D., Lämmle, M., Theis, D., Schneider, S., Frey, G., 2019. Performance modeling of PVT collectors: Implementation, validation and parameter identification approach using TRNSYS. Sol. Energy 193, 51–64. https://doi.org/10.1016/j.solener.2019.09.047

Kabir, E., Kumar, P., Kumar, S., Adelodun, A.A., Kim, K.H., 2018. Solar energy: Potential and future prospects. Renew. Sustain. Energy Rev. 82, 894–900. https://doi.org/10.1016/j.rser.2017.09.094

Karakaya, E., Sriwannawit, P., 2015. Barriers to the adoption of photovoltaic systems: The state of the art. Renew. Sustain. Energy Rev. 49, 60–66. https://doi.org/10.1016/j.rser.2015.04.058

LowUP [WWW Document], 2020. . Low valued energy sources Upgrad. Build. Ind. uses. URL http://lowup-h2020.eu/ (accessed 8.12.20).

Ma, T., Yang, H., Zhang, Y., Lu, L., Wang, X., 2015. Using phase change materials in photovoltaic systems for thermal regulation and electrical efficiency improvement: A review and outlook. Renew. Sustain. Energy Rev. 43, 1273–1284. https://doi.org/10.1016/j.rser.2014.12.003

Mahamudul, H., Rahman, M., Metselaar, H.S.C., Mekhilef, S., Shezan, S.A., Sohel, R., Bin, S., Karim, A., Nur, W., Badiuzaman, I., 2016. Temperature Regulation of Photovoltaic Module Using Phase Change Material : A Numerical Analysis and Experimental Investigation. Int. J. Photoenergy 1–8.

Parida, B., Iniyan, S., Goic, R., 2011. A review of solar photovoltaic technologies. Renew. Sustain. Energy Rev. 15, 1625–1636. https://doi.org/10.1016/j.rser.2010.11.032

Preet, S., Bhushan, B., Mahajan, T., 2017. Experimental investigation of water based photovoltaic/thermal (PV/T) system with and without phase change material (PCM). Sol. Energy 155, 1104–1120. https://doi.org/10.1016/j.solener.2017.07.040

REN21, 2020. Renewables 2020 Global Status Report, Renewable Energy Policy Network for the Century 21. Paris, France.

REN21, 2017. Renewables 2017: Global Status Report, Renewable Energy Policy Network for the Century 21. Paris.

Sarwar, J., Mccormack, S., Huang, M.J., Norton, B., Engineering, E., 2011. Experimental Validation of CFD modelling for thermal regulation of Photovoltaic Panels using Phase Change Material, in: International Conference for Sustainable Energy Storage. Belfast, Ireland, pp. 21–24.

Simón-Allué, R., Guedea, I., Villén, R., Brun, G., 2019. Experimental study of Phase Change Material influence on different models of Photovoltaic-Thermal collectors. Sol. Energy 190, 1–9. https://doi.org/10.1016/j.solener.2019.08.005

Yang, X., Sun, L., Yuan, Y., Zhao, X., Cao, X., 2018. Experimental investigation on performance comparison of PV/T-PCM system and PV/T system. Renew. Energy 119, 152–159. https://doi.org/10.1016/j.renene.2017.11.094